Combination of Neural Networks and DFT Calculations for the Comprehensive Analysis of FDMPO Radical Adducts from Fast Isotropic Electron Spin Resonance Spectra

ARTICLE *in* THE JOURNAL OF PHYSICAL CHEMISTRY A · JANUARY 2012

Impact Factor: 2.69 · DOI: 10.1021/jp203491r · Source: PubMed

5 AUTHORS, INCLUDING:

Katerina Makarova
Medical University of Warsaw
10 PUBLICATIONS **50** CITATIONS
SEE PROFILE

Ekaterina V Rokhina
Temple University
19 PUBLICATIONS **301** CITATIONS
SEE PROFILE

Elena Golovina
Wageningen University
57 PUBLICATIONS **1,422** CITATIONS
SEE PROFILE

Henk Van As
Wageningen University
142 PUBLICATIONS **2,650** CITATIONS
SEE PROFILE

THE JOURNAL OF PHYSICAL CHEMISTRY A

ARTICLE

pubs.acs.org/JPCA

Combination of Neural Networks and DFT Calculations for the Comprehensive Analysis of FDMPO Radical Adducts from Fast Isotropic Electron Spin Resonance Spectra

Katerina Makarova,*[,†,‡] Ekaterina V. Rokhina,[‡] Elena A. Golovina,[‡] Henk Van As,[‡] and Jurate Virkutyte[§]

[†]Faculty of Pharmacy, Department of Physical Chemistry, Medical University of Warsaw, Zwirki i Wigury 61, 02-091 Warsaw, Poland

[‡]Laboratory of Biophysics and Wageningen NMR Centre, Wageningen University, Dreijenlaan 3, 6703 HA Wageningen, The Netherlands

[§]Pegasus Technical Services Inc., 46 East Hollister Street, Cincinnati, Ohio 45219, United States

ABSTRACT: The 4-hydroxy-5,5-dimethyl-2-trifluoromethyl-pyrroline-1-oxide (FDMPO) spin trap is very attractive for spin trapping studies due to its high stability and high reaction rates with various free radicals. However, the identification of FDMPO radical adducts is a challenging task since they have very comparable Electron Spin Resonance (ESR) spectra. Here we propose a new method for the analysis and interpretation of the ESR spectra of FDMPO radical adducts. Thus, overlapping ESR spectra were analyzed using computer simulations. As a result, the N- and F-hyperfine splitting constants were obtained. Furthermore, an artificial neural network (ANN) was adopted to identify radical adducts formed during various processes (e.g., Fenton reaction, cleavage of peracetic acid over MnO_2, etc.). The ANN was effective on both "known" FDMPO radical adducts measured in slightly different solvents and not a priori "known" FDMPO radical adducts. Finally, the N- and F-hyperfine splitting constants of ·OH, ·CH_3, ·CH_2OH, and $CH_3(C{=}O)O$· radical adducts of FDMPO were calculated using density functional theory (DFT) at the B3LYP/6-31G(d,p)//B3LYP/6-31G++//B3LYP/EPR-II level of theory to confirm the experimental data.

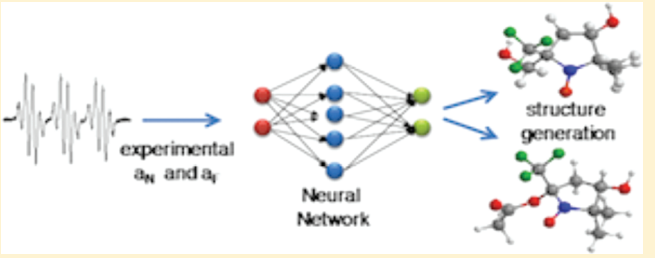

INTRODUCTION

The production of free radicals is essential in normal metabolism. However, in unregulated concentrations, they may cause cell injury or even death.[1] A complete understanding of biological mechanisms that involve free radicals requires efficient radical detection and therefore accurate characterization. Electron Spin Resonance (ESR) spectroscopy has been extensively used for the detection and identification of short-lived free radicals. However, the short lifetime, the high reactivity, and, as a consequence, low concentration of free radicals limit their direct detection. To overcome these drawbacks, the spin trapping method was introduced.[2] It is based on the trapping of radicals by a spin trap, leading to the formation of a more stable radical, a so-called spin adduct, that can be easily detected by ESR spectroscopy. Moreover, the shape of the ESR spectra of a spin adduct can be used to identify the trapped radical. Currently, the spin trapping technique is widely used to study in vitro and in vivo formation of free radicals.[3]

Unfortunately, the use of the spin trapping technique to investigate radical formation in complex systems (e.g., biological systems) faces two important limitations: (1) a different trapping efficiency of particular types of radicals and (2) a short lifetime of some spin adducts (e.g., superoxide).[4] To overcome these limitations, a number of novel spin traps have been introduced and evaluated for qualitative analysis of radical-generating systems. For instance, 4-hydroxy-5,5-dimethyl-2-trifluoromethylpyrroline-1-oxide (FDMPO), a fluorinated analogue of 5,5-dimethylpyrroline-*N*-oxide (DMPO), has already demonstrated effectiveness in assessing radical production due to the high stability of the adducts (up to several days) and the high trapping rate for a wide range of free radicals (including C-centered, ·OH, $O_2{\cdot}^-$, and other free radicals).[5,6] Also, high FDMPO spin-trapping efficiency and its application to the trapping of oxygen and C-centered free radicals in chemical and biological systems have been studied previously.[5] Nonetheless, the identification of FDMPO radical adducts is a challenging task since the relation between the structure and the ESR spectral parameters (splitting pattern) for FDMPO spin adducts is not unique. In most cases, the different radical adducts exhibit very comparable splitting patterns: a triplet of which each line is split in a 1:4:4:1 quartet due to the interaction of the electron spin with the nuclear spins of the nearby N- and F-nuclei. Structural assignment of spectral components can be based on comparison of the ESR parameters of spin adducts produced in alternate ways, e.g., in different solvents.[7] However, the differences between the spin adducts may be insignificant, and the changes in the ESR parameters due

Received: April 14, 2011
Revised: August 23, 2011
Published: October 27, 2011

to a change in the solvent may be larger than the differences between the various radicals.[7,8]

These aforementioned drawbacks are important in complex biological systems if more than one type of radical is generated. In that case, the measured ESR spectrum is a linear superposition of the spectra of the different spin adducts. Such a superposition of overlapping spectra often causes difficulties for qualitative and quantitative analysis of the ESR spectra and complicates the direct extraction of hyperfine splitting constants. Such multicomponent ESR spectra can be analyzed with the aid of simulation-based fitting (SBF), which allows the most accurate extraction of hyperfine splitting constants. In this approach, the experimental ESR spectrum is approximated by a simulated one via mathematical modeling. The choice of the mathematical model for simulation determines which parameters are obtained after the fit and their accuracy. A fast isotropic motion model is successfully used for the simulation of the ESR spectra of various spin traps.[9,10] The difference between experimental and simulated spectra is characterized by an error function or the residuals. So the goal of SBF is to minimize the error function (or residuals) by adjusting ESR parameters, such as hyperfine splitting constants (a_{iso}), g_{iso}, correlation time, and fractions of the components. The experimental and simulated spectra are cyclically compared until the error function is minimal. The set of ESR parameters, which corresponds to the minimum error, is used to identify the trapped radical. This type of analysis is generally performed by a special program (e.g., EasySpin toolbox for Matlab[11,12] or similar programs[12,13]).

An alternative approach to identify radical adducts is the comparison between the theoretical ESR parameters calculated on the basis of Density Functional Theory (DFT) optimized geometries and the experimental ESR parameters of the studied radical adduct.[14] DFT calculations allow us both to estimate the structure of the trapped radical and to predict its ESR spectral parameters, such as hyperfine splitting constants and g_{iso}. The prediction of spin densities and N-hfsc values for various compounds bearing a nitroxyl moiety, for example, nitronyl nitroxides, pyrrolidine *N*-oxides, and piperidine *N*-oxide, has been reported using computational DFT methods. Good agreement with experiments was achieved for DEPMPO and DMPO radical adducts and TEMPO using DFT calculations at the B3LYP, PBE level of theory.[15−17] The computed parameters depend on the molecular geometry, method, and basis set of the calculation. In addition, both solvent and vibrational effects influence the hyperfine splitting constants of a molecule by a few percent regarding the nonvibrating gas phase values. In extreme cases, solvent effects may introduce 10% deviations and vibrational effects (large amplitude motions) deviations as large as 37%.[17] Solvent effects can be approximated by taking into account the Polarized Continuum Model (PCM) with the inclusion of several solvent molecules;[16] however, vibrational effects are expensive to calculate.[17] Thus, it is more practical to determine trends in the dependence of the calculated hyperfine splitting constants on structure and solvent than to compare absolute values with experimental results.[16]

Despite the continuing improvement of accuracy and speed of DFT calculations, there is still a need for the new strategy to identify radical adducts. Key aspects for a new identification method are its applicability to a large number of radical adducts and its robustness to solvent effects on hyperfine splitting constants. However, the correlation between ESR parameters and FDMPO radical adduct structure is hard to express explicitly. The artificial neural network (ANN) approach[18,19] is a powerful tool for approximating functions. Herein, we explore its applicability for FDMPO radical adduct identification utilizing ESR parameters. Due to its flexibility in dealing with different types of input data and nonlinearity, ANNs have been successfully applied to a variety of classification, pattern-recognition, and function-approximation tasks in industry, business, and science.[20,21] Unlike the standard methods for function approximation, the ANN approach does not require the exact specification of a specific function. In ANNs, the synaptic connections between neurons are represented by the numerical weights, which measure the strength of a connection, and by a transfer function that emulates the firing of the neuron. The training of a network involves the establishment of a set of numerical weights that successfully connect the training input (FDMPO adduct hyperfine splitting constants) to the desired output (a predefined group of radicals). Once being trained, ANN can be an effective and rapid tool to identify unknown radical adducts formed in a specific reaction.

Therefore, the goal of the present work was to develop a new comprehensive approach for the analysis of ESR spectra from FDMPO spin adducts to identify trapped radicals. This approach combines simulation of experimental ESR spectra from FDMPO spin adducts and identification of radical adducts by ANN, based on obtained N- and F-hyperfine splitting constants (hfsc). To support spin adduct identification, theoretical DFT calculations were performed. The proposed approach was applied to the analysis of FDMPO spin adducts generated during Fenton reaction in DMSO, methanol, and ethanol and cleavage of the powerful disinfectant, peracetic acid (PAA), over MnO_2. Optimized geometries and theoretical ESR parameters were reported for FDMPO/OH, FDMPO/CH_3, FDMPO/CH_2OH, and FDMPO/CH_3COO radical adducts.

MATERIALS AND METHODS

ESR Spectra Simulation. An SBF approach was used to analyze the ESR spectra. The fast isotropic motion model[22] was used to simulate ESR spectra from FDMPO spin adducts and to extract relevant parameters. The superimposed ESR spectrum arises from different FDMPO radical adducts in the same media, resulting in triplets of which each line is split in a 1:4:4:1 quartet. In this case, changes in the hyperfine splitting constant values (a_F and a_N) and g_{iso} are attributed only to the radical adduct structure. The radical adduct geometry also influences the rotational correlation time τ_R, which defines the broadening of the ESR line shape. The additional broadening of the ESR line shape, originating from the presence of paramagnetic oxygen, influences all the spectral lines of various components in the same way, and therefore only one parameter, Γ_Γ, is needed to describe it. The experimental ESR line shape was described by a Voigtian line shape (a convolution of a Gaussian and Lorentzian line shape with a 1:1 ratio). A fitting program, based on the simplex optimization method of Nearled and Mead,[23] was employed to extract the g-factor, nitrogen, and fluorine hyperfine splitting parameters as well as the rotational correlation time and the fraction of each radical adduct component.

Neural Network Modeling. A small artificial neural network was programmed with Matlab R2009a software using the "newp" routine. A multilayer feed-forward neural network, also known as a multilayer perceptron (MLP),[24] was used in this study. This is a fully connected neural network since a neuron in any layer of the network is connected to all the neurons/nodes of the

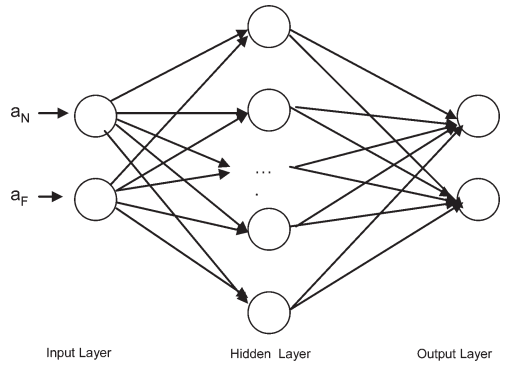

Figure 1. Multilayer perceptron with one hidden layer.

previous layer. The output signals from the first layer form the input signals for the output layer. The layers between the input and output layers are known as hidden layers, and neurons are called hidden neurons. An MLP with sigmoid activation functions[25] and one hidden layer was used. A simple scheme of the network structure and the behavior is shown in Figure 1. The N- and F-hfsc values were used as input for the ANN. The output of the ANN is a predefined group of the radical adducts with similar structure. In the current study, four groups of radical adducts were predefined. The use of a combination of 1 and 0 signals for the ANN output results enabled the use of only two output nodes for the coding of the four groups, i.e., group 1 corresponded to the [0;0] output of the ANN, group 2 to [1,0], group 3 to [0,1], and group 4 to [1,1]. The MLP was trained by the back-propagation algorithm (BPA).[26] During the neural network learning process, the weights of the connections were adjusted by the backward propagation of the error signals at the output of the neural network, layer by layer, until the error between the predicted outputs and the actual outputs was minimized to the target value, Sum Squared Error (SSE) of 0.001.[27]

Training and Testing Data Sets. The data sets for training and validating the neural network model consisted of input data, i.e., nitrogen and fluorine hyperfine splitting constants, and the corresponding output data, i.e., the group of relevant radical adducts. The input data contained nitrogen and fluorine hyperfine splitting constants reported by Khramtsov et al.[5] for the FDMPO spin trap and were extended with data published by Janzen et al.[7] for 5,5-dimethyl-2-(trifluoromethyl)-1-pyrroline *N*-oxide (2-TFDMPO). Hydrogen hyperfine splitting constants were not included as parameters since spectra from radical adducts where hydrogen hyperfine constants could be extracted were not considered for the classification problem. For a better performance of the neural network, the input data were scaled in the interval [0; 1] to avoid higher input values (nitrogen hyperfine splitting constants) having a higher weight in the learning process in comparison to the smaller input values (fluorine hyperfine splitting constants). The neural network was trained on F- and N-hfsc values of 2-TFDMPO spin adducts (Tables 1 and 2-TFDMPO), and the performance of the trained ANN was tested on data not presented in the training set (Table 1, FDMPO).

DFT Calculations. To obtain independent support for the interpretation of ESR spectra, quantum chemistry calculations using density functional theory (DFT) were performed on a set of FDMPO radical adducts to acquire F-hfcs and N-hfcs values. All calculations were carried out using the GAUSSIAN 09 program.[28]

Table 1. Training and Testing Set of Input (Hyperfine Splitting Constants of Various FDMPO and 2-TFDMPO Spin Adducts) and Output (Groups of Radical Adducts) Data

a_N	a_F	group	radical adduct
		FDMPO[a] testing set	
13.9	2.75	2	·OH
14.9	2.05	4	$\cdot CH_3$
14.75	2.4	3	$\cdot CH_2OH$
		2-TFDMPO[b] training set	
13.14	2.8	1	$O_2.^-$
13.98	2.7	2	·OH
14.37	2.64	3	$HOCH_2CH.OH$
14.47	2.87	3	$HOCH.CH_3$
14.52	2.74	3	$HO.CHCH_2CH_3$
14.42	2.33	3	$\cdot CH_2OH$
14.9	2.05	4	$\cdot CH_3$
14.32	2.93	3	$CH_3CH_2CH^{\bullet}OH$
14.91	1.76	4	$\cdot C{\equiv}HC$
13.14	2.8	1	·OOH

[a] Data from Khramtsov et al. 2001 [5]. [b] Data form Janzen et al. 1995 (Janzen, Zhang et al. 1995).

Table 2. Results of FDMPO Radical Adduct Groups Identified by the ANN[a]

experimental			ANN output	
a_N, G	a_F, G	system	group	radical adduct
13.6	2.77	Fenton reaction in methanol	2	·OH
14.08	2.13	Fenton reaction in methanol	3	$\cdot CH_2OH$
13.6	2.7	Fenton reaction in ethanol	2	·OH
14.1	2.59	Fenton reaction in ethanol	3	$HOCH.CH_3$
13.7	2.59	Fenton	2	·OH
14.6	1.93	Fenton reaction in DMSO	4	$\cdot CH_3$
13.7	2.68	Fenton reaction in DMSO	2	·OH
13.8	2.46	PAA	3	$CH_3COO.$
13.7	2.6	PAA	2	·OH

[a] The input values of experimental hyperfine splitting constants were obtained by SBF of ESR spectra of various FDMPO spin adducts from Fenton reaction in methanol, ethanol, and DMSO and the PAA/MnO_2 system.

Optimized geometries of FDMPO/·OH, FDMPO/$\cdot CH_3$, FDMPO/$\cdot CH_2OH$, and FDMPO/$CH_3COO\cdot$ radical adducts were obtained with DFT at the B3LYP/6-31G(d,p) level of theory. Stationary points for geometry optimization of FDMPO radical adducts were determined to have zero imaginary vibrational frequencies as derived from a harmonic vibrational frequency analysis at the level of theory at which the geometries were optimized. The charge and spin density distribution were obtained from the Mullekin population analysis at the B3LYP/EPR-II level of theory.

The atomic coordinates of the geometry optimized radicals were subsequently used to perform a scan over the dihedral angle of the trifluoromethyl group and the pyrroline ring. For each dihedral angle (rotation of CF_3), the total energy and the F-hfcs and N-hfcs were calculated with the B3LYP/EPR-II//B3LYP/6-31++G basis sets. The solvent effect on the hyperfine splitting values was considered using the polarizable continuum model

dx.doi.org/10.1021/jp203491r |*J. Phys. Chem. A* 2012, 116, 443–451

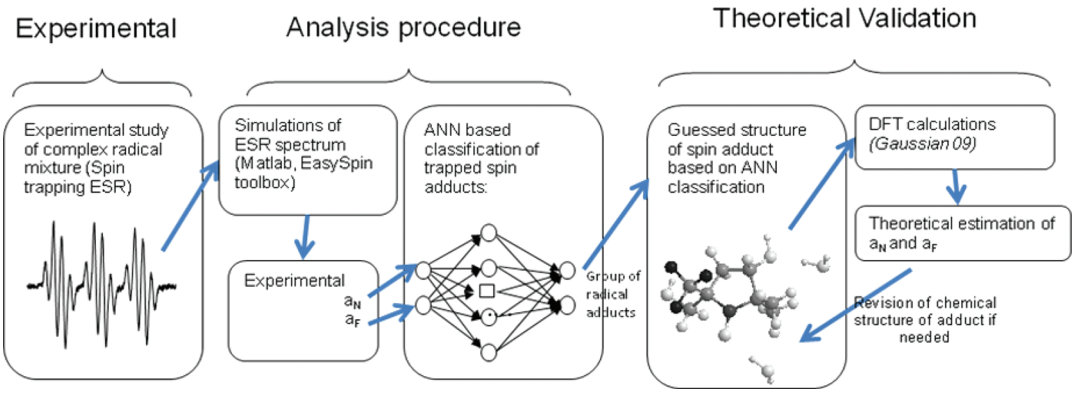

Figure 2. General algorithm for FDMO radical adducts identification.

(PCM) to include the effect of the solvent dielectric constant and two solvent molecules to incorporate the effect of hydrogen bonding.[16,29]

Sample Preparation. MnO_2, PAA (40%), EDTA, methanol, ethanol, DMSO, and other chemicals were purchased from Sigma Aldrich and Merck & Co., Inc. FDMPO was purchased from Alexis Biochemicals (USA). All chemicals were of laboratory reagent grade and were used without further purification. Distilled water was used in all the experiments. The Fenton reaction was carried out using 5 μL of 0.5 mM $FeSO_4$ and 5 μL of 5 mM H_2O_2. The samples were prepared by adding 5 μL of 10 mM FDMPO and 5 μL of ethanol or methanol.

ESR Measurements. ESR measurements were carried out using an X-band Bruker E500 Elexsys SuperX spectrometer with 100 kHz field modulation. Typical instrument settings were 5 mW microwave power, 0.5 G modulation amplitude, 20 s time constant, and four accumulated scans.

RESULTS AND DISCUSSION

General Procedure. The use of computational approaches such as artificial neural networks and quantum chemistry calculations (e.g., DFT methods) allows the interpretation of the complex spectrum obtained for the multicomponent radical systems. ANN provides fast assignment of an unknown radical adduct to the predefined group with similar structure. It could be applied for the variety of biological systems where a number of previously unknown radical adducts could be formed. If no details or no exact structure of the radical adduct are needed, the procedure can be stopped. On the contrary, the accurate DFT calculations are generally applied to the known radical adduct structure to get more information about geometry and the spin density distribution of an adduct. Thus, the use of the DFT calculations to identify previously unknown radical adducts is complicated since all the possible spin adduct structures should be considered.

The proposed algorithm for the analysis of a complex ESR spectrum of FDMPO radical adducts is shown in Figure 2. The general procedure of radical adduct identification consists of three steps: experimental, analysis, and theoretical validation. In the analytical step, the ESR spectrum, obtained experimentally, is simulated by the SBF technique to extract relevant spectral parameters (a_N and a_F). Then, the ANN programming is performed to classify the obtained radical adducts according to the extracted parameters. At this stage, initial structures of the radicals present in the reaction mixture are identified. The analysis procedure could be supplemented by the theoretical validation of the predicted structures. The validation procedure involves the computational (DFT) approach, which allows the computation of the spectral parameters for the proposed structure with high accuracy. If needed, the last step (structure guess) is repeated until the satisfactory agreement between the experimental and theoretical parameters is obtained. The practical application of this algorithm is described below.

Analysis Procedure. *ESR Spectra Simulation.* A number of free radicals systems such as Fenton reaction in DMSO, methanol, and ethanol and the PAA cleavage over heterogeneous MnO_2 were tested. The obtained ESR spectra can be seen in Figure 3. For these systems, the ESR spectral shapes resulted from the superposition of at least two spectra originating from two different radical species. The generated free radical species were characterized by the hyperfine splitting constants from fluorine and nitrogen atoms of FDMPO, F-hfsc (a_F), and N-hfsc (a_N), respectively. Unfortunately, these parameters could not be extracted directly from the experimental spectra due to the spectral overlap. For an accurate interpretation of the experimental spectra of FDMPO radical adducts and the identification of the trapped radicals, the SBF technique was performed. On the basis of SBF, different components in the experimental ESR spectra (Figure 3) were separated on the basis of the N- and F-hfsc values. In general, the simulated spectra (Figure 3, spectra b) were in good agreement with the experimental ones (Figure 3, spectra a), indicating that the proposed model for spectra simulations[22] that considered only the nitrogen complete hyperfine splitting tensor and the g-tensor could be used for the simulation of X-band ESR spectra of the FDMPO radical adducts. The fits allowed us to extract the fraction coefficient f for the two FDMPO spin adducts and the isotropic nitrogen and fluorine hyperfine splitting constants (a_N and a_F) (Figure 3, spectra d,e). The fraction coefficient was defined as the ratio of the integrated intensity of one of the spectral components and the total integrated intensity of the ESR spectrum.

According to the SBF, the hyperfine coupling constants determined for one of the radical adducts for studied systems were in the range of 2.60−2.77 G for a_F and 13.6−13.7 G for a_N (Table 2). The hyperfine coupling constants of the second radical adduct (Figure 3, spectra e) were 1.93−2.6 G for a_F and 13.8−14.6 G for a_N. The next step was the assignment of the FDMPO adduct structure according to the obtained hyperfine coupling constants.

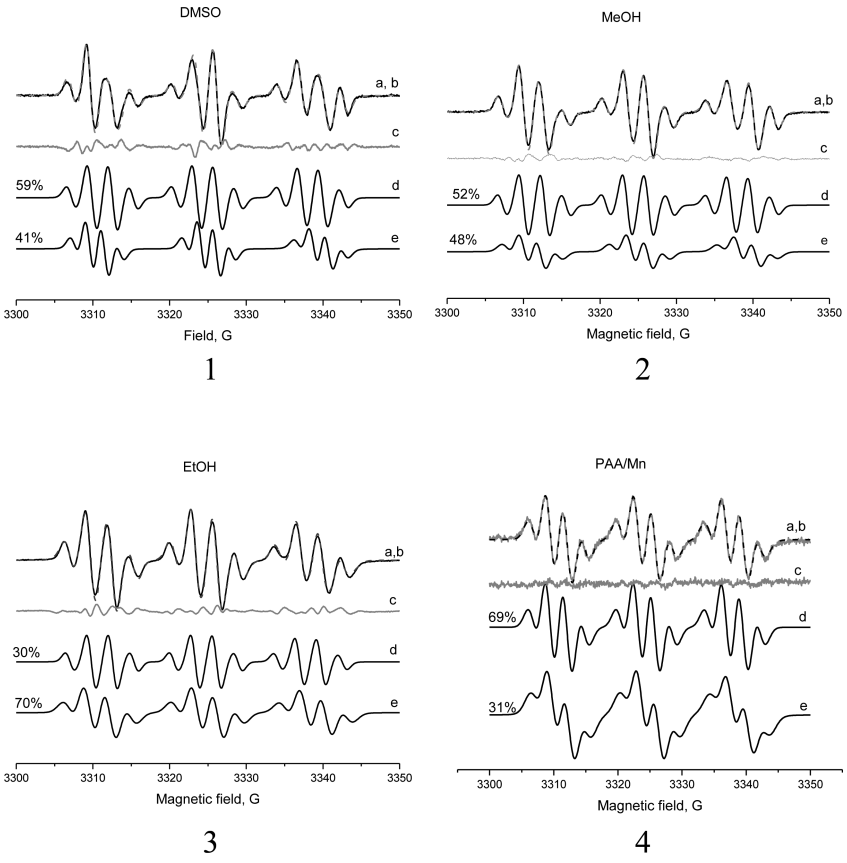

Figure 3. Experimental and simulated spectra of FDMPO spin adducts. (1) DMSO; (2) methanol; (3) ethanol; (4) PAA cleavage over MnO_2. (a, b) Experimental and simulated spectrum of the FDMPO radical adducts; (c) residuals; (d) FDMPO/·OH radical adduct component; (e) C-centered FDMPO radical adduct component.

Development of ANN for Identification of Radical Adducts. Traditionally, for the majority of spin traps, the assignment of radical adducts is based on the formation of the same adducts from known sources. However, sometimes the available spectral parameters do not vary enough to provide the structural information about groups attached further away than two or three bonds from the nitroxyl group.[30,31] This is valid for FDMPO.[5] The identification of FDMPO trapped radicals is mainly based on the precise hfsc values originating from the spin trap moiety (in particular, the N- and F-hfsc values), which act as spectral fingerprints of the trapped radical. For instance, C-centered radical adducts have larger N-hfsc values than oxyl adducts.[5,31] In addition, the magnitude of F-hfsc can also be a useful marker for the identification of the FDMPO spin adducts, though it is not likely to vary in an easily predictable manner.

Therefore, the primary goal of the development of an ANN was to create an effective tool to correlate N- and F-hfsc values with the structure of the radical adducts. So, experimental N- and F-hfsc values of numerous radical adducts were used as input for the ANN. The output of the ANN was the predefined group of radical adducts. However, ANN required training prior to the analysis of experimental data. Training a network involved establishing a set of numerical weights that successfully connected *a training input* (FDMPO adduct hyperfine splitting constants) with *a desired output* (predefined group of radicals).

ANN Training and Testing Input Sets Construction. To provide a systematic approach to classify radical adducts according to their chemical structure, several representative FDMPO radical adducts with well-determined parameters were taken from previously published data[5] (Table 1). However, the data set was too small for the efficient training of ANN, so the training set was extended with a hyperfine splitting constant of 2-TFDMPO.[7] Noteworthy, the chemical structure of the 2-TFDMPO spin trap was similar to that of FDMPO. Therefore, the hyperfine splitting constants corresponding to the same radical adducts had similar values. For example, a_N = 13.9 and a_F = 2.75 of FDMPO/·OH were very comparable to a_N = 14.0 and a_F = 2.7 of 2-TFDMPO/·OH, as well as hyperfine splitting constants of FDMPO/·CH_3 (a_N = 14.6 G and a_F = 2.05 G) and 2-TFDMPO/·CH_3 (Figure 4, Table 1).

Moreover, in the case of FDMPO and 2-TFDMPO, the variation of nitrogen and fluorine hyperfine splitting of radical adducts provides structural information mainly about the group attached not further away than three to four bonds from the nitrogen and fluorine atoms (e.g., CH, CO, OH, and OO). The free radical groups can be described qualitatively as electron-donating groups or electron-withdrawing groups.[32] Spin adducts with electron-donating free radicals favor a positive imbalance of spin density on ^{14}N and exhibit larger N-hfsc values, whereas spin adducts with progressively stronger electron-withdrawing groups have smaller N-hfsc values and a smaller positive imbalance of spin density on ^{14}N. This effect was studied for PBN-nitronyl-C^{13} adducts,[33] which exhibited larger N-hfsc values in the case of a nonpolar ·CH_3 radical adduct and smaller N-hfsc values in the case of an ·OH radical adduct.

In addition to the chemical structure information, N- and F-hfsc values also reflect the polarity and proticity of the radical

dx.doi.org/10.1021/jp203491r |*J. Phys. Chem. A* 2012, 116, 443–451

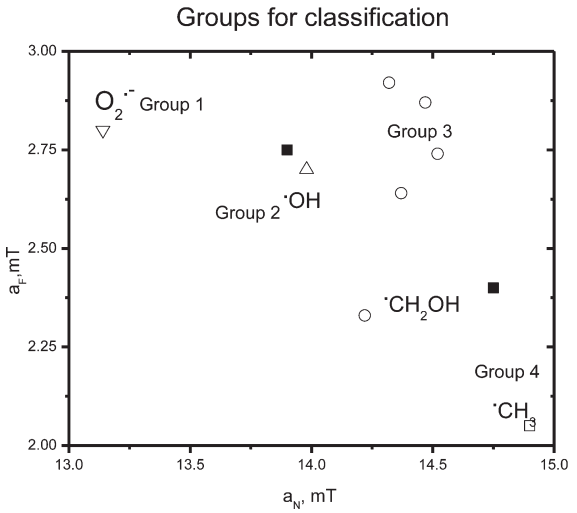

Figure 4. Plot of a_F vs a_N for groups of 2-TFDMPO (open symbols) and FDMPO (filled squares) radical adducts based on published F- and N-hfsc values.[5,7]

adduct environment. Generally, there is an increase in the N-hfsc with an increase in the polarity of the solvent.[16] Indeed, the N-hfsc value reported for the 2-TFDMPO/CH_2═CH· spin adduct in water solvent (ε = 79) was 1.5 G higher than the N-hfsc value in benzene (ε = 2.27).[7] In the case of Fenton reaction in water and Fenton reaction in DMSO, ethanol, and methanol, the changes in the polarity were rather small,[34,35] so only a small variation of the N-hfsc values was expected.

ANN Output Construction (Grouping of Radicals on the Basis of Spectral Parameters According to the Chemical Structure). In Figure 4, a_F has been plotted against a_N for several FDMPO and 2-TFDMPO radical adducts (data from Table 2). There were four groups based on a similar electronegative character of the free radical group attached to the carbon-2 atom:

Group 1 (coded as [0,0] output of ANN) contained oxygen $O^{2\cdot-}$ and ·OOH radicals.

Group 2 (coded as [1,0] output of ANN) included only the hydroxyl (·OH) radical where oxygen was combined with hydrogen. The radical adducts in groups 1 and 2 with two electronegative (polar) groups attached to carbon-2 gave relatively small N-hfsc values (Table 1). Radical adducts from group 2 (·OH) and group 1 ($O^{2\cdot-}$ and ·OOH) spin adducts could be separated based on N-hfsc values since hydroxyl N-hfsc values were about 0.8 G larger than those of superoxide spin adducts. F-hfsc values were insensitive to changes in the trapped-radical structure with a 0.1 G difference between the two groups.

Group 3 (coded as [0,1] output of ANN) included carbon−oxygen radical adducts with a CO (alkoxyl) group attached to carbon-2, i.e., hydroxymethyl radical (·CH_2OH), 1-hydroxyethyl radical (·CH_3CHOH), etc. For this group, only a small variation was found in the N-hfsc values with different radical adduct structure, although the variation in F-hfsc values was ca. 0.6 G. The N-hfsc values of this group were 0.5 G smaller than of group 4 and 0.5−1.5 G larger than the N-hfsc values of the first and the second group.

Group 4 (coded as [1,1] output of ANN) included radicals with the largest N-hfsc and the smallest F-hfsc values as well as the carbon-centered spin adducts without oxygen (e.g., ·CH3 and CH≡C·). The N-hfsc values in the same solvents were ca. 1−1.8 G larger and the F-hfsc values ca. 0.7 G smaller in comparison to those from ·OH and $O^{2\cdot-}$ spin adducts.

Results of ANN Modeling. An MLP with one hidden layer consisting of 55 nodes was always accurate enough to identify the group of similar FDMPO radical adduct structures based on the experimental N- and F-hfsc values. The network was trained with the training set for around 600 iterations, until the sum of squares for error (SSE) between the desired and actual output of ANN reached its lowest point (0.001). Due to its ability to generalize, ANN trained on the 2-TFDMPO data set performed well on the testing set of hyperfine splitting constants of FDMPO radical adducts from Table 1.

The main advantage of classification obtained in the current ANN modeling is its applicability to a free radical with unknown structure but known hpf's, which makes the analysis of systems generating a new type of free radicals or systems in different solvents with FDMPO easier.

Identification of the Radical Adducts in the Experimental ESR Spectra of FDMPO with Developed ANN. The F- and N-hfsc values extracted from the experimental ESR spectra of FDMPO spin adducts formed during Fenton reaction in DMSO and methanol and in the PAA cleavage over MnO_2 (Table 2) were analyzed with developed ANN. These experimental data contained additional details which were not captured in the training set. It included imperfect knowledge of the hyperfine splitting constants due to the simulation error (0.05 G) and the different polarity of the solvents used. It was reported that the polarities of water/DMSO,[34] water/ethanol, and water/methanol mixtures were slightly lower ($\varepsilon \sim 70$) than those of pure water (ε = 79). The MLP algorithm, used in the current ANN modeling, was very robust and capable of dealing with both indicated problems. The first radical adduct with N- and F-hfsc values in the range of 13.6−13.74 G and 2.59−2.84 G, respectively, was recognized by ANN as FDMPO/OH in all the studied systems (Table 2). The other radical adducts with 1.93−2.6 G and 3.8−14.6 G N- and F-hfsc values, respectively, were recognized as carbon centered radicals. The C-centered radical adduct from Fenton reaction with DMSO was assigned to group 4 and was associated with the FDMPO/·CH_3 spin adduct. The C-centered radical adducts observed during Fenton reaction in methanol and ethanol, FDMPO/·CH_2OH and FDMPO/·CH_3CH_3OH, were successfully assigned by the MLP to group 3. The C-centered spin adduct observed in the PAA/MnO_2 system, namely, FDMPO/CH_3COO·, was also assigned to group 3. The final assignment of the radical structure was completed by the theoretical validation.

Theoretical Validation. DFT calculations were used to predict ESR parameters based on the chemical structure of a radical adduct. The B3LYP/EPR-II//B3LYP/6-31G(d,p)//B3LYP/6-31++G level of theory has been previously employed to predict N-hfsc for various nitronyl nitroxides, and findings were in a good agreement with experimental values.[15]

Calculation of a_N. Figure 5 shows the optimized structures together with the obtained values of a_N and a_F which are strongly dependent on the computation level. For all spin adducts, the calculation at the level B3LYP/6-31++G gave the values of a_N close to the experimental ones, whereas another approach (B3LYP/EPR-II) led to underestimated N-hfsc's. Moreover, N-hfsc values obtained at the B3LYP/6-31++G level of theory followed the general trend; i.e., FDMPO spin adduct with progressively stronger electron-withdrawing radicals (−OH) exhibited smaller N-hfsc values (14.0 G), while FDMPO with an electron-donating group (−CH_3) exhibited an N-hfsc of 14.2 G.

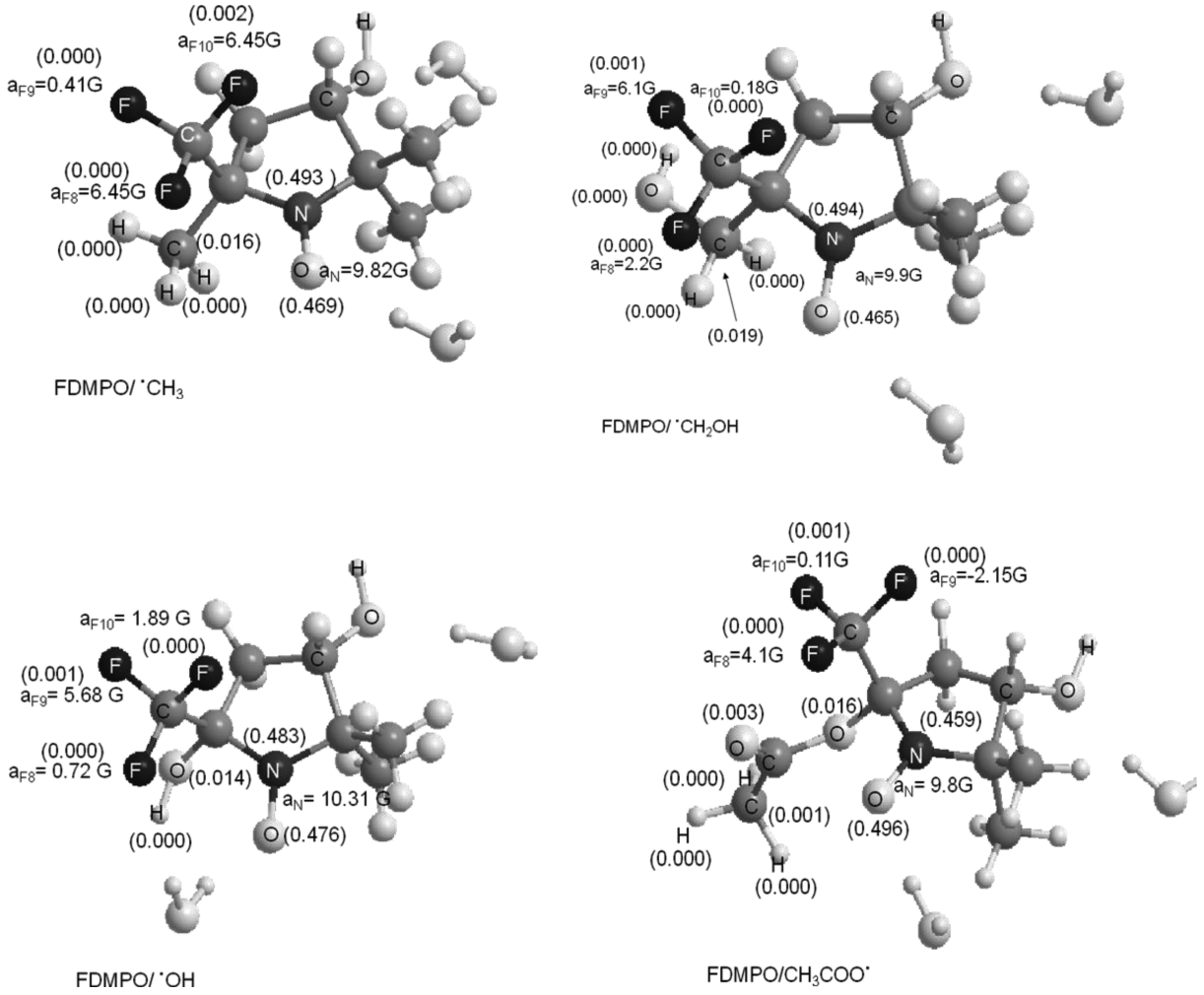

Figure 5. F and N hyperfine splitting constant values and spin populations of ·CH_3, ·OH, ·CH_2OH, and CH_3COO· spin adducts of the FDMPO spin trap and two water molecules calculated at the B3LYP/EPR-II level of theory. F and N hyperfine splitting constant values calculated at the B3LYP/6-31++G level of theory are shown in parentheses.

In contrast, N-hfsc values calculated at the B3LYP/EPR-II level of theory did not follow the general pathway resulting in a_N values of 10.3 and 9.8 G for FDMPO/·OH and FDMPO/·CH_3, respectively (Figure 5). To explain the findings, spin density calculations were performed since the decrease (increase) of the spin density on the N atom resulted in the decrease (increase) of a_N value.

Spin Density Analysis. The calculated spin density (B3LYP/EPR-II) was mainly localized on the nitroxide fragment (NO), whereas the spin densities of the pyrroline ring atoms and the methyl and trifluoromethyl groups were small. As evidenced in Figure 5, the redistribution of the electron spin density induced by the trapped radical structure predominantly occurred in the NO bond. Thus, only the nitroxide fragment of the FDMPO spin adducts was considered in more detail. Due to variation in radical adduct structure, the total spin density (sum of N and O spin densities) in the nitroxide fragment slightly decreased from 0.96 to 0.95 for ·CH_3 and ·OH radicals, respectively.

Qualitative interpretation of the spin density distribution in the nitroxide group was based on the two main resonance structures >N−O· (1) and $>N^+.-O^-$ (2), which differed with respect to the localization of an unpaired electron.[36] An electron-donating group (−CH_3) added electron density to the system and stabilized the resonance structure (2) resulting in an increase in the spin density on N (0.49). In contrast, an electron-withdrawing group (−OH) removed electron density from the system and led to the resonance structure (1) causing a decrease in the spin density of the N atom (0.48).

Also, the geometry of FDMPO could change depending on the trapped radical. It was reported[36] that these changes could affect the values of the N-hfcs, so a_N would not be strictly proportional to the spin density in the case of B3LYP/EPR-II calculations.

Calculations of Rotationally Averaged a_F. Interestingly, the DFT calculations resulted in three different values of a_F for the trifluoromethyl group (0.72, 5.68, and 1.89 G for FDMPO/·OH as shown at Figure 5). This could be attributed to the fact that DFT calculations took into consideration only one orientation of the trifluoromethyl group. Whereas in an experimental system the trifluoromethyl group was allowed to rotate freely, the F-hfsc values were averaged, resulting in the typical spectrum of a triplet, of which each line was split into a quartet with a 1:4:4:1 intensity ratio.[7] However, when the rotation of the CF_3 group was limited due to the interaction with a solvent or with the trapped radical, the spectrum would change dramatically. The phenyl adduct of 2-TFDMPO[7] exhibited an entirely different type of spectrum

dx.doi.org/10.1021/jp203491r |*J. Phys. Chem. A* 2012, 116, 443–451

Table 3. Hyperfine Splitting Constants of Various FDMPO Spin Adducts from DFT Calculations at the B3LYP/6-31++G and B3LYP/EPR-II Levels of Theory Using the PCM Model for Water Solvent and Two Water Molecules

	a_N, G		a_F, G	
FDMPO radical adduct	EPR-II	6-31++G	EPR-II	6-31++G
$\cdot CH_3$	9.8	14.3	3.1	2.5
$\cdot CH_2OH$	9.9	14.2	2.8	2.9
$\cdot OH$	10.4	13.9	2.9	3.2
$CH_3COO\cdot$	9.6	13.5	1.7	1.9

that consisted of three groups of doublets with unresolved peaks mainly due to three different F-hfsc values.

To improve the results of the single-point calculation, the dihedral angle of the trifluoromethyl group and pyrroline ring was changed, allowing only the rotation of the trifluoromethyl group, as similarly done for bisdi(trifluoromethyl) nitroxide.[37] For each dihedral angle, the single-point calculations of the hyperfine splitting constants were performed using the B3LYP/EPR-II//B3LYP/6-31++G level of theory. Subsequently, the Maxwell−Boltzman distribution was applied to calculate numerical values of the rotationally averaged hyperfine couplings. The total energy of the optimized geometries, E_{tot}, was used to determine the probability, p, assuming that the radical adduct existed in a certain conformation with a specific dihedral angle φ

$$p(\varphi) = \frac{\exp\left(-\frac{E_{tot}(\varphi)}{kT}\right)}{\sum_{\varphi=0}^{120} \exp\left(-\frac{E_{tot}(\varphi)}{kT}\right)} \quad (1)$$

These probabilities were used to weight the contribution of the hfsc at that particular angle to calculate the averaged isotropic hyperfine coupling constants via the mean value expression

$$\langle a_{iso} \rangle = \sum_{\varphi=0}^{120} p(\varphi) a_{iso}(\varphi) \quad (2)$$

Subsequently, the averaged values from the CF_3 group were used for comparison with experimental values. Importantly, rotation of the CF_3 group significantly influenced N-hfcs. The rotation averaged values of a_N and a_F were presented in Table 3. Indeed, the averaging over the dihedral angle drastically improved the results of hyperfine splitting calculations. The averaged values of F-hfsc calculated at the B3LYP/EPR-II level of theory were only slightly overestimated by 0.2, 0.5, and 1 G for FDMPO/$\cdot OH$, FDMPO/$\cdot CH_2OH$, and FDMPO/$\cdot CH_3$ radical adducts, respectively, in comparison to the experimental values from Table 2. Moreover, the calculation of the same values at the B3LYP/6-31++g level of theory resulted in 0.5−0.7 G overestimated values for all the FDMPO radical adducts.

Thus, in the case of the functional B3LYP, the use of the basis set 6-31++G provided better results to calculate N-hfsc. The spectral parameters calculated at this level of theory were used to support the results of ANN analysis. However, calculations of spectral parameters at the B3LYP/EPR-II level of theory were not accurate enough to identify spin adducts even when motional effect of the trifluoromethyl group and solvent effects were accounted. The further improvements (i.e., corrections for >N−O$^{\cdot}$ fragment vibrations or the use of relaxed scan for each dihedral angle of the trifluoromethyl group[37]) could provide more accurate results in the computations of spectral parameters at this level of theory.

CONCLUSIONS

This study demonstrated that a combination of computer simulation based fitting of ESR spectra, ANN, and DFT calculations allowed a comprehensive analysis of FDMPO radical adducts. Computer simulations were used for the decomposition of the ESR spectra and extraction of relevant hyperfine splitting constants. Then, ANN-based identification was used for preliminary estimation of the radical adduct chemical structure. Finally, the chemical structure could be verified by DFT calculations of hyperfine splitting constants.

This approach is potentially important for the analysis of multicomponent free radical systems with a variety of free radicals. The approach outlined here can easily be generalized to other radical adducts which exhibits overlapping ESR spectra. Moreover, the proposed approach was used to identify free radicals observed during Fenton reaction in methanol, ethanol, DMSO, and the PAA cleavage over MnO_2 in water. The ANN performed well with experimental data and tolerated the solvent effect on N- and F-hyperfine splitting constants. To verify the results of ANN identification, DFT calculations of the minimum energy geometry of $\cdot OH$, $\cdot CH_3$, $\cdot CH_2OH$, and $CH_3OO\cdot$ radical adducts of FDMPO spin trap have been performed.

AUTHOR INFORMATION

Corresponding Author

*E-mail: kmakarova@wum.edu.pl. Telephone: +48 22 5720958. Fax: +48 22 572 09 51.

ACKNOWLEDGMENT

This research was supported by the European Community activity Large-Scale Facility Wageningen NMR Center (FP6-2004-026164 (2006−2009)). The DFT calculations were performed with the Gaussian 03 package in the Interdisciplinary Centre for Mathematical and Computational Modeling (Warsaw, Poland) under the computational Grant G14-6.

REFERENCES

(1) Blake, D. R.; Allen, R. E.; Lunec, J. *Braz. Med. Bull.* **1987**, *43*, 371.
(2) Janzen, E. G. *Acc. Chem. Res.* **1971**, *4*, 31.
(3) Dikalova, A. E.; Kadiiska, M. B.; Mason, R. P. *Proc. Natl. Acad. Sci. U.S.A.* **2001**, *98*, 13549.
(4) Finkelstein, E. L. I.; Rosen, G. M.; Rauckman, E. J.; Paxton, J. *Mol. Pharmacol.* **1979**, *16*, 676.
(5) Khramtsov, V. V.; Reznikov, V. A.; Berliner, L. J.; Litkin, A. K.; Grigor'ev, I. A.; Clanton, T. L. *Free Radical Biol. Med.* **2001**, *30*, 1099.
(6) Bacic, G.; Spasojevic, I.; Secerov, B.; Mojovic, M. *Spectrochim. Acta, Part A* **2008**, *69*, 1354.
(7) Janzen, E. G.; Zhang, Y.-K.; Arimura, M. *J. Org. Chem.* **1995**, *60*, 5434.
(8) Janzen, E. G. Spin trapping. In *Foundations of modern EPR*; Eaton, G. R., Eaton, S. S., Salikhov, K. M., Eds.; World Scientific: Singapore, 1998.
(9) Busi, E.; Travagli, V.; Zanardi, I.; Gabbrielli, A.; Basosi, R. *Appl. Magn. Reson.* **2010**, *37*, 325.
(10) Rokhina, E. V.; Makarova, K.; Golovina, E. A.; Van As, H.; Virkutyte, J. *Environ. Sci. Technol.* **2010**, *44*, 6815.
(11) Stoll, S.; Schweiger, A. *J. Magn. Reson.* **2006**, *178*, 42.

(12) Budil, D. E.; Lee, S.; Saxena, S.; Freed, J. H. *J. Magn. Reson.* **1996**, *120*, 155.
(13) Kirste, B. *Anal. Chim. Acta* **1992**, *265*, 191.
(14) Jerzykiewicz, M.; Cwielag-Piasecka, I.; Witwicki, M.; Jezierski, A. *Chem. Phys. Lett.* **2010**, *497*, 135.
(15) Villamena, F. A.; Hadad, C. M.; Zweier, J. L. *J. Am. Chem. Soc.* **2004**, *126*, 1816.
(16) Owenius, R.; Engstrom, M.; Lindgren, M.; Huber, M. *J. Phys. Chem. A* **2001**, *105*, 10967.
(17) Fau, S.; Bartlett, R. J. *J. Phys. Chem. A* **2003**, *107*, 6648.
(18) Bishop, C. M. *Neural networks for pattern recognition*; Oxford University Press, Inc.: Oxford, 1995.
(19) Wasserman, P. D. *Neural computing: theory and practice*; Van Nostrand Reinhold: New York, 1989.
(20) Corne, S. A.; Johnson, A. P.; Fisher, J. *J. Magn. Reson.* **1992**, *100*, 256.
(21) Roth, M. W. *IEEE Trans. Neural Network* **1990**, *1*, 28.
(22) Israelachvili, J.; Sjösten, J.; Eriksson, L. E. G.; Ehrström, M.; Gräslund, A.; Ehrenberg, A. *Biochim. Biophys. Acta* **1975**, *382*, 125.
(23) Nelder, J. A.; Mead, R. *Comp. J.* **1965**, *7*, 308.
(24) Rosenblatt, F. *Psychol. Rev.* **1958**, *65*, 386.
(25) Mitchell, T. M. Artificial Neural Networks. In *Machine learning*; McGraw-Hill, Inc.: New York, 1997; Vol. 1.
(26) Rumelhart, D. E.; Hinton, G. E.; Williams, R. J. *Nature* **1986**, *323*, 533.
(27) William, M. *Introduction to probability and statistics*, 7th ed.; Duxbury Press: Boston, MA, 1986.
(28) Frisch, M. J.; Trucks, G. W.; Schlegel, H. B.; Scuseria, G. E.; Robb, M. A.; Cheeseman, J. R.; Montgomery, J. A.; Vreven, T.; Kudin, K. N.; Burant, J. C.; Millam, J. M.; Iyengar, S. S.; Tomasi, J.; Barone, V.; Mennucci, B.; Cossi, M.; Scalmani, G.; Rega, N.; Petersson, G. A.; Nakatsuji, H.; Hada, M.; Ehara, M.; Toyota, K.; Fukuda, R.; Hasegawa, J.; Ishida, M.; Nakajima, T.; Honda, Y.; Kitao, O.; Nakai, H.; Klene, M.; Li, X.; Knox, J. E.; Hratchian, H. P.; Cross, J. B.; Bakken, V.; Adamo, C.; Jaramillo, J.; Gomperts, R.; Stratmann, R. E.; Yazyev, O.; Austin, A. J.; Cammi, R.; Pomelli, C.; Ochterski, J. W.; Ayala, P. Y.; Morokuma, K.; Voth, G. A.; Salvador, P.; Dannenberg, J. J.; Zakrzewski, V. G.; Dapprich, S.; Daniels, A. D.; Strain, M. C.; Farkas, O.; Malick, D. K.; Rabuck, A. D.; Raghavachari, K.; Foresman, J. B.; Ortiz, J. V.; Cui, Q.; Baboul, A. G.; Clifford, S.; Cioslowski, J.; Stefanov, B. B.; Liu, G.; Liashenko, A.; Piskorz, P.; Komaromi, I.; Martin, R. L.; Fox, D. J.; Keith, T.; Laham, A.; Peng, C. Y.; Nanayakkara, A.; Challacombe, M.; Gill, P. M. W.; Johnson, B.; Chen, W.; Wong, M. W.; Gonzalez, C.; Pople, J. A. *Gaussian 03*, revision C.02; Gaussian, Inc.: Wallingford, CT, 2004.
(29) Tomasi, J.; Mennucci, B.; Cammi, R. *Chem. Rev.* **2005**, *105*, 2999.
(30) Smirnova, T. I.; Smirnov, A. I.; Clarkson, R. B.; Belford, R. L.; Kotake, Y.; Janzen, E. G. *J. Phys. Chem. B.* **1997**, *101*, 3877.
(31) Janzen, E. G.; Liu, G. *J. Magn. Reson.* **1973**, *9*, 513.
(32) Church, D. F. *J. Org. Chem.* **1986**, *51*, 1138.
(33) Haire, L. D.; Krygsman, P. H.; Janzen, E. G.; Oehler, U. M. *J. Org. Chem.* **1988**, *53*, 4535.
(34) Yang, L.-J.; Yang, X.-Q.; Huang, K.-M.; Jia, G.-Z.; Shang, H. *Int. J. Mol. Sci.* **2009**, *10*, 1261.
(35) Harvey, A. H.; Prausnitz, J. M. *J. Solution Chem.* **1987**, *16*, 857.
(36) Improta, R.; Barone, V. *Chem. Rev.* **2004**, *104*, 1231.
(37) Mattar, S. M.; Sanford, J. *J. Phys. Chem. A* **2009**, *113*, 11435.